

# Ground-State Phase Diagram of Frustrated Antiferromagnetic $S = 1$ Chain with Uniaxial Single-Ion-Type Anisotropy

Toshiya HIKIHARA\*

*National Institute for Materials Science, Tsukuba, Ibaragi 305-0047*

(Received December 30, 2021)

The ground-state phase diagram of a frustrated  $S = 1$  Heisenberg spin chain with uniaxial single-ion-type anisotropy is studied using the infinite-system density-matrix renormalization-group method. Particular attention is paid to “chiral” phases, in which the long-range order parameter is a vector chirality. It is found that, in addition to the Haldane, large-D (LD), and double-Haldane phases, the phase diagram includes three different chiral phases, i.e., the gapless chiral, chiral-Haldane, and chiral-LD phases. These chiral phases are distinguished from each other by the energy gap and the string long-range order.

**KEYWORDS:** frustration, spin-1 chain, ground-state phase diagram, uniaxial single-ion-type anisotropy, chiral ordering, density-matrix renormalization-group method

## §1. Introduction

The effect of geometrical frustration in quantum spin systems has attracted considerable attention for many years. Frustration generally suppresses the tendency towards the classical Néel ordering and leads to a wide variety of exotic phenomena such as a spontaneous breaking of the translational symmetry in a one-dimensional (1D) system and spin-liquid states in 2D and 3D systems. Among them, the possibility of a novel “chiral” phase in 1D frustrated quantum spin systems has been studied intensively in recent years.<sup>1, 2, 3, 4, 5, 6, 7)</sup> This chiral phase is characterized by the absence of the helical long-range order (LRO),

$$\mathbf{m}(q) = \frac{1}{LS} \sum_l \mathbf{S}_l e^{iql} = 0 \quad (\text{for } \forall q), \quad (1.1)$$

and the non-zero value of the  $z$ -component of the total vector chirality,<sup>8)</sup>

$$\begin{aligned} O_\kappa &= \frac{1}{LS^2} \sum_l \kappa_l \neq 0, \\ \kappa_l &= S_l^x S_{l+1}^y - S_l^y S_{l+1}^x = [\mathbf{S}_l \times \mathbf{S}_{l+1}]_z, \end{aligned} \quad (1.2)$$

---

\* E-mail address: HIKIHARA.Toshiya@nims.go.jp

where  $\mathbf{S}_l$  is a spin- $S$  operator at site  $l$  and  $L$  is the system size assumed to be even throughout this paper. The chiral phase breaks only the parity symmetry spontaneously with preserving the time-reversal and translational symmetries. Using the bosonization method, Nersisyan *et al.* predicted the appearance of the chiral phase in the frustrated antiferromagnetic  $S = 1/2$  chain with nearest-neighbor and next-nearest-neighbor couplings of easy-plane anisotropy.<sup>1)</sup> From the analytical<sup>2,3)</sup> and numerical<sup>4,5,6)</sup> studies, it has been shown that the chiral phase appears in the frustrated chain with the anisotropic couplings in general spin- $S$  cases. The ground-state phase diagrams for the  $S = 1/2, 1, 3/2$ , and  $2$  cases have been determined numerically.<sup>5,6)</sup>

Another interesting observation in the studies<sup>3,4,5,6)</sup> is that *there exist two different chiral phases* in the integer- $S$  cases. One of them is the “chiral-Haldane” phase where the chiral LRO coexists with the string LRO<sup>9,10)</sup>

$$O_{\text{str}} = \frac{1}{LS} \sum_l \exp \left( \sum_{k=1}^{l-1} i \frac{\pi}{S} S_k^z \right) S_l^z, \quad (1.3)$$

which characterizes the well-known Haldane phase,<sup>11,12)</sup> and the spin correlation function decays exponentially with a finite energy gap. The other is the “gapless chiral” phase where the chiral LRO exists and the spin and string correlation functions decay algebraically with gapless excitations. It has been shown that for  $S = 1$  and  $2$  the gapless chiral phase exists in a broad region of the ground-state phase diagrams while the chiral-Haldane phase exists in a narrow region between the Haldane and gapless chiral phases. (See Fig. 1 in ref. 5 and Fig. 9 in ref. 6.) For  $S = 1/2$  and  $3/2$ , on the other hand, the gapless chiral phase exists as in the integer- $S$  cases while the chiral phase with a finite energy gap has not been identified.

As the mechanism generating the chiral phases, easy-plane anisotropy plays an essential role as well as frustration does. The anisotropy lowers the symmetry of the system from  $SU(2)$  to  $U(1) \times Z_2$  and induces a two-fold discrete degeneracy according as the right- and left-handed chirality. In fact, the chiral phases do not appear in the isotropic case where the discrete chiral degeneracy no longer exists. From the experimental viewpoint, the anisotropy in real materials commonly takes the form of the uniaxial single-ion-type. It is therefore important to study the effect of the single-ion-type anisotropy on the chiral phases, for the sake of exploring experimental implications of the theoretical results and stimulating an investigation into the chiral phases in real materials. Nevertheless, most of the theoretical findings on the chiral phases mentioned above have been obtained for the case of the anisotropic exchange couplings. Kolezhuk<sup>3)</sup> studied recently the frustrated integer- $S$  spin chain with the single-ion-type anisotropy by means of a large- $S$  approach and presented a schematic phase diagram including the gapless chiral phase and a chiral phase with a finite energy gap. However, systematic studies on the chiral phases in the case of single-ion-type anisotropy have been scarce so far.

The aim of this paper is to investigate the ground-state properties of the frustrated  $S = 1$

Heisenberg chain with the uniaxial single-ion-type anisotropy. The model Hamiltonian is given by

$$\mathcal{H} = \sum_{\rho=1,2} \left\{ J_{\rho} \sum_l \mathbf{S}_l \cdot \mathbf{S}_{l+\rho} \right\} + D \sum_l (S_l^z)^2. \quad (1.4)$$

I concentrate on the case of the antiferromagnetic couplings ( $J_1 > 0$  and  $J_2 > 0$ ) and the easy-plane anisotropy ( $D > 0$ ). Hereafter I denote  $j \equiv J_2/J_1$  and  $d \equiv D/J_1$ . The ground-state properties of the model (1.4) have been studied for some limiting cases. For  $j = 0$  the phase transition between the Haldane and large-D (LD) phases have been studied intensively.<sup>13,14,15,16</sup> It has been found that as  $d$  increases the system undergoes a continuous phase transition from the Haldane phase to the LD phase at  $d = 1.000 \pm 0.001$ .<sup>16</sup> Meanwhile, it has been shown for  $d = 0$  that as  $j$  increases the system undergoes a first order transition at  $j \simeq 0.747$  from the Haldane phase to the “double Haldane” (DH) phase,<sup>5,17,18</sup> in which the next-nearest-neighbor coupling  $J_2$  becomes dominant so that the system is described as two Haldane subchains weakly coupled by the inter-subchain coupling  $J_1$ . The string LRO vanishes discontinuously at the transition. Furthermore, the appearance of the gapless and gapped chiral phases has been predicted by the large- $S$  approach.<sup>3)</sup>

In the present work, I determine numerically the ground-state phase diagram of the model (1.4) by employing the same method as the one used in our previous works.<sup>4,5,6)</sup> I calculate the appropriate correlation functions associated with the order parameters characterizing each phase using the density-matrix renormalization group (DMRG) method,<sup>19,20)</sup> and then, analyze their long-distance behaviors. From the obtained phase diagram, we find that the gapless chiral phase appears in a broad region of the  $j$ - $d$  plane while the chiral-Haldane phase appears in a narrow region between the Haldane and gapless chiral phases, which are essentially the same as those in the case of the anisotropic exchange couplings. It is found further that, in addition to the gapless chiral and chiral-Haldane phases, another novel chiral phase exists between the gapless chiral and LD phases. This “chiral-LD” phase is characterized by the chiral LRO and the exponential decay of both the spin and string correlation functions.

The paper is organized as follows. In §2, I introduce the chiral, string, and spin correlation functions associated with each order parameter and explain the numerical method. The obtained phase diagram and numerical data are presented in §3. The results are summarized in §4.

## §2. Correlation Functions and Numerical Method

The method used to determine the phase diagram is essentially the same as those used in our previous works.<sup>4,5,6)</sup> I have calculated the two-point chiral, string, and spin correlation functions defined by

$$C_{\kappa}(l, l') = \langle \kappa_l \kappa_{l'} \rangle, \quad (2.1)$$

$$C_{\text{str}}(l, l') = \langle S_l^z \exp \left( i\pi \sum_{k=l}^{l'-1} S_k^z \right) S_{l'}^z \rangle, \quad (2.2)$$

$$C_s^x(l, l') = \langle S_l^x S_{l'}^x \rangle, \quad (2.3)$$

which are associated with the order parameters (1.2), (1.3), and (1.1), respectively. The notation  $\langle \cdots \rangle$  represents the expectation value in the lowest energy state in the subspace of  $S_{\text{total}}^z = \sum_l S_l^z = 0$  with even parity. It has been checked by the exact-diagonalization calculation that the ground state of the chain indeed belongs to the subspace. The calculation has been performed for various fixed values of  $d(j)$  with varying  $j(d)$ . Then, I have estimated the transition points  $j_c(d_c)$  by examining the dependence of the correlation functions on  $r = |l - l'|$  at long distance.

I have employed the infinite-system DMRG algorithm originally introduced by White<sup>19,20)</sup> and accelerated it by making use of the recursion relation proposed by Nishino and Okunishi.<sup>21,22)</sup> The number of kept states  $m$  is up to 350 if not otherwise mentioned. The convergence of the data with respect to  $m$  has been checked by increasing  $m$  consecutively. Since the truncation error of the DMRG calculation increases dramatically as  $j$  increases, the calculation is limited to rather small  $j$ . However, I consider that the region of  $j$  treated in this work,  $j \lesssim 1$ , is enough to study the properties of the chiral phases which we wish to know. In the calculations, the open boundary condition has been imposed for the sake of the best performance of the algorithm. Accordingly, in order to avoid the unwanted boundary effect, the two-point correlation functions have been calculated for the sites  $l$  and  $l'$  near the center of the chain, i.e.,  $l = l_0 - r/2$  and  $l' = l_0 + r/2$  where  $l_0 = L/2$  for even  $r$  and  $l_0 = (L + 1)/2$  for odd  $r$ . By checking the convergence of the data with increasing  $L$  typically up to 2000, I have confirmed that the data are free from the effect of the open boundaries.

### §3. Phase Diagram

By examining the long-distance behaviors of the chiral, string, and spin correlation functions introduced in the previous section, I have determined the ground-state phase diagram of the model (1.4) in the  $j$ - $d$  plane. The obtained phase diagram shown in Fig. 1 includes six different phases, i.e., the Haldane, LD, DH, gapless chiral, chiral-Haldane, and chiral-LD phases. The long-distance behaviors of the correlation functions in each of the phases are summarized in Table I. We can see in Fig.1 that the gapless chiral phase appears in a broad region of the phase diagram while the chiral-Haldane phase appears between the Haldane and gapless chiral phases. Further we find the chiral-LD phase, where the chiral LRO exists while the spin and string correlation decay exponentially, between the LD and gapless chiral phases. Two multi-critical points, at least, are observed: One of them is at  $(j_{M1}, d_{M1}) \simeq (0.51, 0.76)$  among the Haldane, LD, gapless chiral, chiral-Haldane, and chiral-LD phases while the other is at  $(j_{M2}, d_{M2}) \simeq (0.75, 0.15)$  among the Haldane, gapless chiral, chiral-Haldane and DH phases. The numerical data for each transition line are discussed in the following subsections.

### 3.1 Haldane-chiral transition

First let us consider the phase transitions between the Haldane and chiral phases. Figures 2(a)-(c) show the data of the chiral, string, and spin correlation functions in log-log plots for  $d = 0.5$  and several typical values of  $j$ . The data of the spin correlation shown in Fig. 2 (c) are divided by the leading oscillating factor  $\cos(Qr)$  where  $Q$  is the wavenumber characterizing the incommensurate oscillation of  $C_s^x(r)$  in real space. It can be clearly seen in Fig. 2 (a) that the data of the chiral correlation function  $C_\kappa(r)$  are bent upward for  $j > j_{c1} \simeq 0.635$  suggesting a finite chiral LRO while they are bent downward for  $j < j_{c1}$  suggesting the absence of the chiral ordering. The transition point where the chiral LRO sets in is estimated to be  $j_{c1} = 0.635 \pm 0.005$ . As shown in Fig. 2 (b), the string correlation function exhibits a finite LRO for  $j < j_{c2} \simeq 0.670$  whereas it decays algebraically for  $j > j_{c2}$ .<sup>23)</sup> Meanwhile, the data of the spin correlation function shown in Fig. 2 (c) are bent downward for  $j < j_{c2}$  suggesting an exponential decay with a finite energy gap while they exhibit a linear behavior for  $j > j_{c2}$  suggesting a power-law decay with gapless excitations. The transition point  $j_{c2}$  where the string LRO and the energy gap vanish is estimated to be  $j_{c2} = 0.670 \pm 0.010$ . It should be noticed that the estimate of  $j_{c2}$  is distinctly larger than that of  $j_{c1}$ . Accordingly, the chiral-Haldane phase where the chiral and string LROs coexist and the spin correlation decays exponentially exists in a narrow but finite region between the Haldane and gapless chiral phases. The existence of the chiral-Haldane phase can be clearly seen from the behavior of the correlation functions at  $j = 0.640$  and  $0.660$  which lie between  $j_{c1}$  and  $j_{c2}$ . Thus, it is concluded that the system undergoes two successive transitions as  $j$  increases, first at  $j = j_{c1}$  from the Haldane phase to the chiral-Haldane phase, and then, at  $j = j_{c2}$  to the gapless chiral phase. The results are essentially the same as the ones observed in the frustrated chain with anisotropic exchange couplings.<sup>4,5)</sup>

Performing calculations in the same manner for various fixed  $d$  ( $j$ ) with varying  $j$  ( $d$ ), I have determined the transition points  $j_{c1}$  ( $d_{c1}$ ) and  $j_{c2}$  ( $d_{c2}$ ) plotted in Fig. 1. The figure may suggest that the transition lines connecting the estimated points run from the multi-critical point  $(j_{M1}, d_{M1})$  to the other multi-critical point  $(j_{M2}, d_{M2})$ . The chiral-Haldane phase is identified for  $d = 0.7, 0.6, 0.5, 0.4$ , and  $0.3$  while it is not for  $d = 0.2$  within the calculation with varying  $j$  at intervals of  $0.002$ . However, I note that it is difficult to exclude the possibility that the chiral-Haldane phase exists in a too narrow region to be detected. Thus it is not clear whether the transition lines  $j_{c1}$  and  $j_{c2}$  merge at  $(j_{M2}, d_{M2})$  or at another multi-critical point  $(j'_{M2}, d'_{M2})$  with  $d'_{M2} > 0.2$ . In the latter case, a transition line  $j'_{c1}$  between the Haldane and gapless chiral phases connects  $(j'_{M2}, d'_{M2})$  and  $(j_{M2}, d_{M2})$ . For  $d = 0.1$  and  $0.05$ , on the other hand, the chiral LRO is not observed. In these cases, it is also found that the string LRO vanishes discontinuously at the transition point and the spin correlation function exhibits an exponential decay for all calculated values of  $j$ . The  $j$  dependence of the string correlation function at  $r \rightarrow \infty$  for  $d = 0.1$  is shown in Fig. 3 together with the spin-correlation length  $\xi$  estimated by fitting the data of  $C_s^x(r)$  to the form of an exponential

decay,  $C_s^x(r) = A \cos(Qr) \exp(-r/\xi)$ , where  $A$  is a numerical constant. These behaviors of the string and spin correlation functions for  $d = 0.1$  and  $0.05$  suggest a first-order transition between two gapful phases, i.e., the Haldane and DH phases. From the observations, it is concluded that between  $d = 0.2$  and  $d = 0.1$  there is a multi-critical point  $(j_{M2}, d_{M2})$  where the transition lines  $j_{c1}$  and  $j_{c2}$  or the transition line  $j'_{c1}$  merges with the DH-chiral transition line discussed in §3.4. The first-order transition line between the Haldane and DH phases smoothly connects the multi-critical point  $(j_{M2}, d_{M2})$  to the transition point in the isotropic case ( $d = 0$ ),  $j_{c2} \simeq 0.747$ , estimated in the previous works.<sup>5,17,18)</sup>

### 3.2 LD-chiral transition

We next consider the phase transitions between the LD and chiral phases. The data of the chiral, string, and spin correlation functions for  $j = 0.8$  and several typical values of  $d$  are shown in Figs. 4 (a)-(c) in log-log plots. As shown in Fig. 4 (a), the chiral correlation function  $C_\kappa(r)$  exhibits a finite LRO for  $d < d_{c3} \simeq 1.09$  while it decays exponentially for  $d > d_{c3}$ . The transition point  $d_{c3}$  where the chiral LRO vanishes is thereby estimated as  $d_{c3} = 1.09 \pm 0.01$ . Meanwhile, the string and spin correlations decay exponentially for  $d > d_{c4} \simeq 0.80$  suggesting a finite energy gap whereas they decay algebraically for  $d < d_{c4}$  suggesting gapless excitations.<sup>23)</sup> The transition point  $d_{c4}$  is estimated to be  $d_{c4} = 0.80 \pm 0.10$ . Unfortunately, the numerical error of the estimate of  $d_{c4}$  is quite large due to the truncation error of the DMRG calculation, which tends to underestimate the string and spin correlation functions. Nevertheless, from the behaviors of the correlation functions for  $0.94 \lesssim d < d_{c3}$ , it can be clearly seen that there exists a intermediate region with a finite chiral LRO and a finite energy gap. In order to confirm the appearance of the intermediate phase, I have performed a high-precision calculation with  $m$  up to 500 for  $d = 1.00$  and  $0.94$ . The data shown in Fig. 4, which are almost free from the truncation error, clearly suggest that the parameter points  $d = 1.00$  and  $0.94$  indeed belong to the chiral phase with a finite energy gap. It is therefore concluded that the estimate of  $d_{c4}$  is distinctly smaller than that of  $d_{c3}$  and the system undergoes two successive transitions as  $d$  decreases, first at  $d = d_{c3}$  from the LD phase to the “chiral-LD” phase characterized by a finite chiral LRO and an exponential decay of the string and spin correlation functions, and then at  $d = d_{c4}$  to the gapless chiral phase. Here it should be noticed that the chiral-LD phase is distinct from the chiral-Haldane phase with respect to the absence of the string LRO. Hence the chiral-LD phase can be regarded as a new type of the gapped chiral phase.

By the same calculation for various fixed  $j$  ( $d$ ), the transition points  $d_{c3}$  ( $j_{c3}$ ) and  $d_{c4}$  ( $j_{c4}$ ) are estimated. In particular, the appearance of the chiral-LD phase has been confirmed by the high-precision calculations with  $m$  up to 500 for the points plotted in Fig. 1 by crosses. As seen in Fig. 1, the chiral-LD phase appears in a finite region between the LD and gapless chiral phases. The transition lines  $d_{c3}$  and  $d_{c4}$  merge with the Haldane-chiral transition lines  $j_{c1}$  and  $j_{c2}$  around the multi-critical point  $(j_{M1}, d_{M1})$  into the Haldane-LD transition line discussed in the next subsection.

### 3.3 Haldane-LD transition

In this subsection, we see the results for the phase transition between the Haldane and LD phases. The phase transition has been studied in detail in the case of no frustration ( $j = 0$ ).<sup>13, 14, 15, 16</sup> It has been pointed out that there occurs a continuous phase transition accompanying the vanishing of the energy gap at  $d = 1.000 \pm 0.001$ . In Figs. 5 (a) and (b), I show the data of the string and spin correlation functions for  $j = 0.2$  and several typical values of  $d$ . Here the  $m$  convergence of the data has almost been achieved even at  $m = 180$ . We can see in Fig. 5 (a) that the string correlation function exhibits a finite LRO for  $d < d_{c5} \simeq 0.90$  while it exhibits an exponential decay for  $d > d_{c5}$ . In the meantime, the spin correlation function exhibits an exponential decay for  $d \leq 0.89$  and  $d \geq 0.91$  in accordance with the existence of a finite energy gap in both phases while it decays algebraically at  $d = 0.90$  suggesting the vanishing of the energy gap at the transition. The transition point between the Haldane and LD phases for  $j = 0.2$  is thereby estimated to be  $d_{c5} = 0.90 \pm 0.01$ . The transition points  $d_{c5}$  estimated in the same way are plotted in Fig. 1. The transition line connecting the estimates runs from the point  $d_{c5} = 0.96 \pm 0.02$  at  $j = 0$ , which is slightly smaller than the previous estimate  $d_{c5}(j = 0) = 1.000 \pm 0.001$ , to the multi-critical point  $(j_{M1}, d_{M1})$ .

### 3.4 DH-chiral transition

Here we consider the phase transition between the DH and chiral phases. Figure 6 (a) shows the chiral correlation function  $C_\kappa(r)$  for  $d = 0.3$  and several typical values of  $j$  around the DH-chiral transition. As shown in the figure,  $C_\kappa(r)$  exhibits a finite LRO for  $j < j_{c6} \simeq 0.820$  while it decays exponentially for  $j > j_{c6}$ . Thus, the transition point where the chiral LRO vanishes is estimated to be  $j_{c6} = 0.820 \pm 0.010$ . Meanwhile, the data of the spin correlation function for  $d = 0.3$  are shown in Fig. 6 (b) where the data are divided by the oscillating factor  $\cos(Qr)$ . It can be seen in the figure that as  $j$  increases the spin correlation changes its behavior from an algebraic decay to an exponential decay at  $j = j_{c7} \simeq 0.780$ . Although the truncation error of the data prevents us from carrying out the precise estimation, the transition point is estimated to be  $j_{c7} = 0.780 \pm 0.040$ .

Here arises a question: Whether  $j_{c7}$  is equal to or smaller than  $j_{c6}$ ? If  $j_{c7}$  is equal to  $j_{c6}$ , there occurs only one phase transition at  $j = j_{c6} = j_{c7}$  between the gapless chiral phase and the DH phase. On the other hand, if  $j_{c7}$  is smaller than  $j_{c6}$ , the system undergoes two successive transitions as  $j$  increases, first at  $j = j_{c6}$  from the gapless chiral phase to an intermediate “chiral-DH” phase with a finite chiral LRO and a finite energy gap, and then at  $j = j_{c7}$  to the DH phase. Unfortunately, the estimates of the transition points, particularly that of  $j_{c7}$ , are not accurate enough to determine which of the cases is realized. Here I note that the data of the spin correlation for  $j = 0.800$  shown in Fig. 6 (b) are calculated with  $m$  up to 500 and still suffer from the truncation error which is not negligible. This means that it is unpromising to achieve the sufficiently accurate estimate of  $j_{c7}$  in the manner used in this work. The difficulty in identifying the intermediate phase in this case can

be ascribed partly to the fact that no order parameter characterizing the DH phase has been found so far<sup>24)</sup> and partly to the fact that the intermediate phase, if any, appears only in a narrow region which can be concealed behind the error bar of  $j_{c7}$ . Hence, the situation here is different from that of the Haldane-chiral transition where we can utilize the string order parameter to estimate  $j_{c2}$  and that of the LD-chiral transition where the region of the chiral-LD phase is so broad that we can identify the chiral-LD phase even with rather rough estimates of  $d_{c4}$ . Since it is a subtle problem to estimate the point where the behavior of the spin correlation changes, it might be needed for the settlement of the question to introduce an order parameter characterizing the DH phase. This problem remains open for future studies.

In the same manner, I have estimated the transition points  $j_{c6}$  and  $j_{c7}$  for  $d = 0.2$  and  $d = 0.4$ . The chiral-DH phase has not been identified also in these cases. As shown in Fig. 1, the transition lines connecting the estimates seem to emerge from the multi-critical point  $(j_{M2}, d_{M2})$ . The values of  $j_{c6}$  and  $j_{c7}$  become larger as  $d$  becomes larger suggesting that the DH phase becomes stable as  $j$  increases.

### 3.5 Multi-critical point

Lastly, I touch upon the region of the phase diagram around the multi-critical point  $(j_{M1}, d_{M1})$ . It can be seen in the obtained phase diagram Fig. 1 that the five transition lines run into a narrow region around  $(j_{M1}, d_{M1})$ . It might be useful to classify them into three groups, i.e., the transition lines  $j_{c1}$  and  $d_{c3}$  where the chiral LRO sets in, the lines  $j_{c2}$  and  $d_{c4}$  between gapful and gapless phases, and the line  $d_{c5}$  between the Haldane and LD phases. Here I note that the mechanism generating the chiral LRO is essentially distinct from the one generating the energy gap<sup>2,3)</sup> and, to my knowledge, no definite relation between them has been known. Thus, the behavior of the chiral transition lines ( $j_{c1}$  and  $d_{c3}$ ) and the “gapful-gapless” lines ( $j_{c2}$  and  $d_{c4}$ ) around the multi-critical point is still nontrivial. Looking at Fig. 1, two possibilities seem to be left: (i) The five transition lines merge at one multi-critical point  $(j_{M1}, d_{M1})$ . (ii) The transition lines  $j_{c1}$  and  $d_{c3}$  merge with the Haldane-LD transition line  $d_{c5}$  at  $(j_{M1}, d_{M1})$  while the lines  $j_{c2}$  and  $d_{c4}$  merge with the transition line  $d'_{c5}$  between the chiral-Haldane and chiral-LD phases at another multi-critical point  $(j'_{M1}, d'_{M1})$ . These scenarios are illustrated in Fig. 7 (a) and (b), respectively. Because of the rather large error of the estimates of  $d_{c4}$  mentioned in §3.2, we can not decide which of the cases is realized from the present numerical results. More detailed studies might be needed to identify the universality class of the multi-critical point(s) and transition lines.

## §4. Summary

In this paper, the ground-state properties of the frustrated  $S = 1$  Heisenberg spin chain with uniaxial single-ion-type anisotropy (eq. (1.4)) have been investigated numerically by the infinite-system DMRG method. By calculating the chiral, string, and spin correlation functions and analyz-



ing their long-distance behaviors, I have determined the ground-state phase diagram for  $0 \leq j \lesssim 1$  and  $d \geq 0$  (Fig. 1). It has turned out that there exist six different phases, namely, the Haldane, LD, DH, gapless chiral, chiral-Haldane, and chiral-LD phases. The gapless chiral phase appears in a broad region of the phase diagram while the chiral-Haldane phase appears in the narrow but finite region between the Haldane and gapless chiral phases; these results are essentially the same as those found in the frustrated  $S = 1$  chain with anisotropic exchange couplings.<sup>4,5)</sup> Meanwhile, the chiral-LD phase has been found between the LD and gapless chiral phases. Since the chiral-LD phase is characterized by a finite chiral LRO, the absence of the string LRO, and the short-range spin correlation function, it is distinct from either the gapless chiral or the chiral-Haldane phase and can be regarded as a new type of the gapped chiral phases. The question about the existence of the possible chiral-DH phase remains open.

After the theoretical finding of the chiral phases, one of the most challenging tasks is the experimental observation of the phases in real materials. As seen in the obtained phase diagram, the anisotropy  $d \gtrsim 0.15$  and the next-nearest neighbor coupling  $j$  within a suitable range around  $j \simeq 0.75$  are required for a material realizing the chiral phases. These values of  $d$  and  $j$  are realistic so that there must be a good chance to find out a material in the parameter region. If such a material is prepared, the measurement of the vector chirality (1.2) is, in principle, possible by using polarized neutrons.<sup>25,26,27)</sup> I hope that the results of the present paper stimulate further experimental studies.

## Acknowledgments

The author is very grateful to M. Kaburagi and H. Kawamura for collaboration in early stage of this work. He also thanks X. Hu for useful discussions. Numerical calculations were carried out in part at Yukawa Institute Computer Facility, Kyoto University. The author was supported by a Grant-in-Aid for Encouragement of Young Scientists from Ministry of Education, Science and Culture of Japan.

- 
- [1] A. A. Nersesyan, A. O. Gogolin and F. H. L. Essler: Phys. Rev. Lett. **81** (1998) 910.
  - [2] P. Lecheminant: T. Jolicoeur and P. Azaria, Phys. Rev. B **63** (2001) 174426 .
  - [3] A. K. Kolezhuk: Phys. Rev. B **62** (2000) R6057.
  - [4] M. Kaburagi, H. Kawamura and T. Hikihara: J. Phys. Soc. Jpn. **68** (1999) 3185.
  - [5] T. Hikihara, M. Kaburagi, H. Kawamura and T. Tonegawa: J. Phys. Soc. Jpn. **69** (2000) 259.
  - [6] T. Hikihara, M. Kaburagi and H. Kawamura: Phys. Rev. B **63** (2001) 174430.
  - [7] Y. Nishiyama: Eur. Phys. J. B **17** (2000) 295.
  - [8] Note that the vector chirality (1.2) differs from the scalar chirality  $\chi_l = \mathbf{S}_{l-1} \cdot \mathbf{S}_l \times \mathbf{S}_{l+1}$  which is often discussed in the context of isotropic spin systems: The vector chirality changes its sign under the parity operation but is invariant under the time-reversal operation whereas the scalar chirality changes its sign under both operations.
  - [9] M. den Nijs and K. Rommelse: Phys. Rev. B **40** (1989) 4709.
  - [10] M. Oshikawa: J. Phys. Condens. Matter **4** (1992) 7469.

- [11] F. D. M. Haldane: Phys. Lett. **93A** (1983) 464.
- [12] F. D. M. Haldane: Phys. Rev. Lett. **50** (1983) 1153.
- [13] U. Glaus and T. Schneider: Phys. Rev. B **30** (1984) 215.
- [14] O. Golinelli, Th. Jolicoeur and R. Lacaze: Phys. Rev. B **46** (1992) 10854.
- [15] T. Tonegawa, T. Nakao and M. Kaburagi, J. Phys. Soc. Jpn. **65** (1996) 3317.
- [16] W. Chen, K. Hida and B. C. Sanctuary: J. Phys. Soc. Jpn. **69** (2000) 237.
- [17] A. Kolezhuk, R. Roth and U. Schollwöck: Phys. Rev. Lett. **77** (1996) 5142.
- [18] A. Kolezhuk, R. Roth and U. Schollwöck: Phys. Rev. B **55** (1997) 8928.
- [19] S. R. White: Phys. Rev. Lett. **69** (1992) 2863.
- [20] S. R. White: Phys. Rev. B **48** (1993) 10345.
- [21] T. Nishino and K. Okunishi: J. Phys. Soc. Jpn. **64** (1995) 4084.
- [22] Y. Hieida, K. Okunishi and Y. Akutsu: Phys. Lett. A **233** (1997) 464.
- [23] The string correlation functions for  $j = 0.680$  and  $0.700$  in Fig. 2 (b) and for  $d = 0.80$  and  $0.70$  in Fig. 4 (b) seem to be bent downward for  $r \gtrsim 40$ . However, I note that the  $m$  convergence of the data for  $r \gtrsim 40$  has not been achieved yet and the string correlation is enhanced as  $m$  increases. Thus, from the behavior of the string correlation for  $r \lesssim 40$  where the  $m$  convergence is almost achieved, I consider that the string correlations for the above  $j$ 's and  $d$ 's exhibit an algebraic decay and the bend-downward behavior observed for larger  $r$  is an artifact due to the truncation error eventually vanishing in the limit  $m \rightarrow \infty$ .
- [24] Since the system in the DH phase can be described as two Haldane subchains, one might expect that the string correlation function on each subchains can be the order parameter of the phase. Contrary to the naive expectation, however, the string correlation on a subchain does not exhibit a finite LRO but decays exponentially. (See refs.17 and 18.)
- [25] M. L. Plumer, H. Kawamura and A. Caillé: Phys. Rev. B **43** (1991) 13786.
- [26] S. V. Maleyev, V. P. Plakhty, O. P. Smirnov, J. Wosnitza, D. Visser, R. K. Kremer and J. Kulda: J. Phys.: Condens. Matter **10** (1998) 951.
- [27] V. P. Plakhty, J. Kulda, D. Visser, E. V. Moskvina and J. Wosnitza: Phys. Rev. Lett. **85** (2000) 3942.

Fig. 1. The ground-state phase diagram of the model (1.4). The circles, squares, and diamonds represent the points where the chiral LRO sets in, the points where the string LRO vanishes, and the points where the behavior of the spin and string correlations changes from an exponential to an algebraic decay. The multi-critical points  $(j_{M1}, d_{M1})$  and  $(j_{M2}, d_{M2})$  are indicated as “M1” and “M2”, respectively. The crosses represent the points for which the calculations with  $m = 500$  are performed. The lines are to guide the eye.

Fig. 2. The  $r$  dependence of the correlation functions for  $d = 0.5$ : (a) chiral correlation  $C_\kappa(r)$ ; (b) string correlation  $-C_{\text{str}}(r)$ ; (c) spin correlation  $C_s^x(r)$  divided by the oscillating factor  $\cos(Qr)$ . The number of kept states is  $m = 350$ . To illustrate the  $m$  dependence, the data with  $m = 260$  and  $300$  are indicated by crosses: for  $j = 0.620$  and  $0.630$  in (a); for  $j = 0.680$  and  $0.700$  in (b). In other cases, the truncation errors are smaller than the symbols. The data of  $C_\kappa(r)$  for  $j = 0.700$  in (a), which are almost the same as those for  $j = 0.680$ , are omitted for clarity.

Fig. 3. The  $j$  dependence of the string correlation function  $-C_{\text{str}}(r)$  at  $r \rightarrow \infty$  (solid circle) and the inverse spin-correlation length  $\xi^{-1}$  (open circle) for  $d = 0.1$ . The dotted line represents the transition point.

Fig. 4. The  $r$  dependence of the correlation functions for  $j = 0.8$ : (a) chiral correlation  $C_\kappa(r)$ ; (b) string correlation  $-C_{\text{str}}(r)$ ; (c) spin correlation  $C_s^x(r)$  divided by the oscillating factor  $\cos(Qr)$ . The number of kept states is  $m = 500$  for  $d = 0.94$  and  $1.00$  while it is  $m = 350$  for the other cases. To illustrate the  $m$  dependence, the data with  $m = 260$  and  $300$  for  $d = 0.80$ , and  $0.70$  are indicated in (b) by crosses. In other cases, the truncation errors are smaller than the symbols.

Fig. 5. The  $r$  dependence of the correlation functions for  $j = 0.2$ : (a) string correlation  $-C_{\text{str}}(r)$ ; (b) spin correlation  $(-1)^r C_s^x(r)$ . The number of kept states is  $m = 180$ . The truncation errors are smaller than the symbols.

Fig. 6. The  $r$  dependence of the correlation functions for  $d = 0.3$ : (a) chiral correlation  $C_\kappa(r)$ ; (b) spin correlation  $C_s^x(r)$  divided by the oscillating factor  $\cos(Qr)$ . The number of kept states is  $m = 500$  for  $j = 0.800$  and  $m = 350$  for other values of  $j$ . To illustrate the  $m$  dependence, the data with smaller  $m$  are indicated by crosses: the data with  $m = 260$  and  $300$  for  $j = 0.820$  in (a); the data with  $m = 350$  and  $400$  for  $j = 0.800$  and with  $m = 260$  and  $300$  for  $j = 0.760$  in (b). In other cases, the truncation errors are smaller than the symbols.

Fig. 7. The possible schematic pictures of the phase diagram around the multi-critical point  $(j_{M1}, d_{M1})$ . Figures (a) and (b) correspond to the cases (i) and (ii) in text, respectively.

Table I. The long-distance behaviors of the spin, chiral, and string correlation functions in each of the phases. The words "expo." and "power" mean an exponential decay and a power-law decay, respectively.

	Haldane	chiral-Haldane	gapless chiral	LD	chiral-LD	DH
$C_s^x$	expo.	expo.	power	expo.	expo.	expo.
$C_\kappa$	expo.	LRO	LRO	expo.	LRO	expo.
$C_{\text{str}}$	LRO	LRO	power	expo.	expo.	expo.

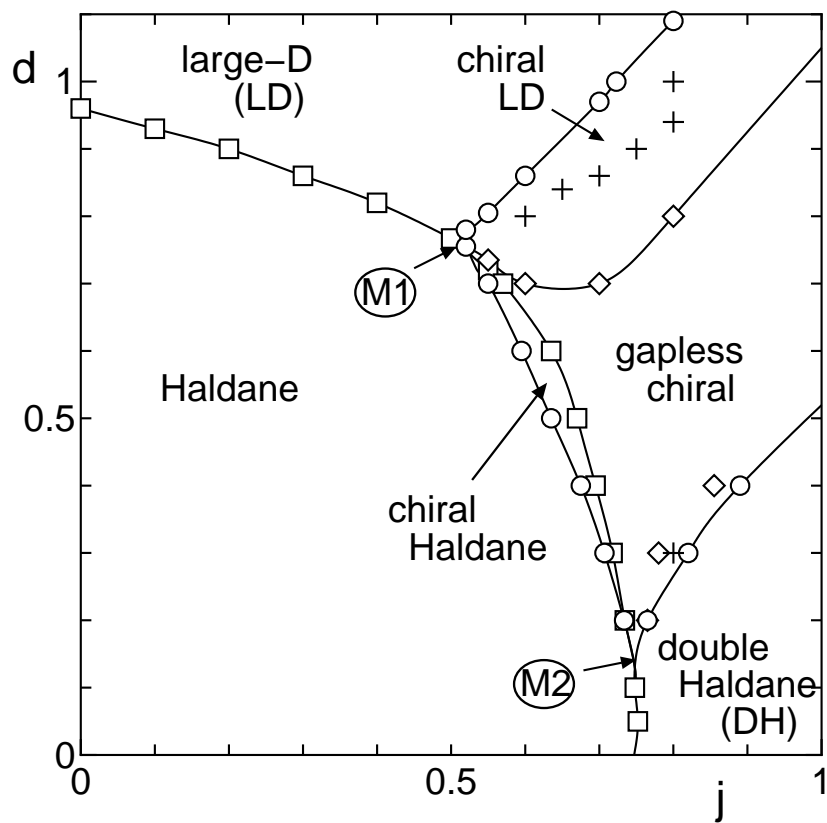


Fig.1, T.Hikihara

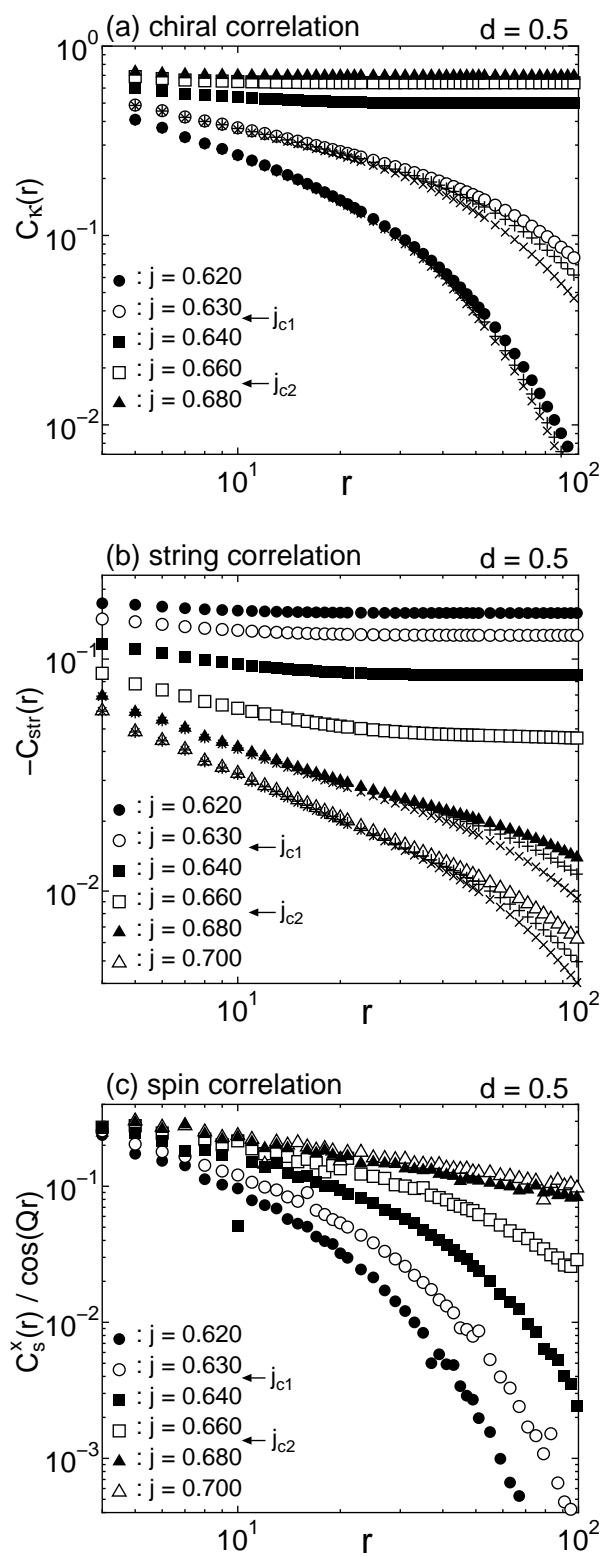


Fig.2, T.Hikihara

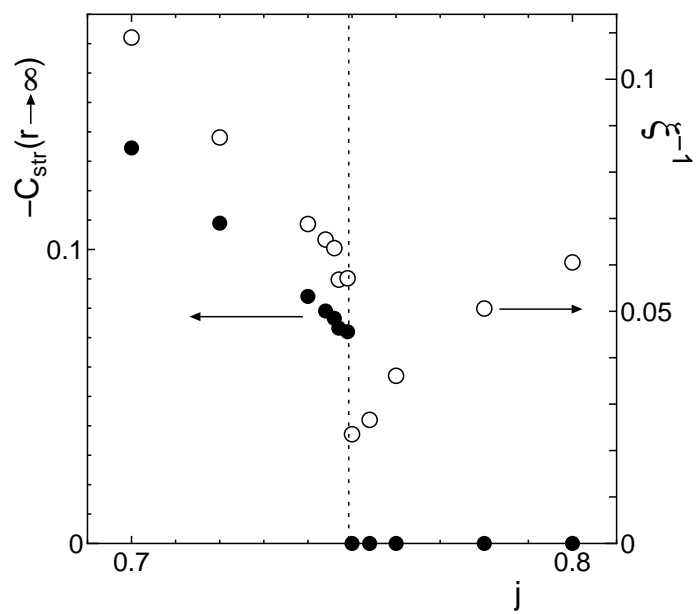


Fig.3, T.Hikihara

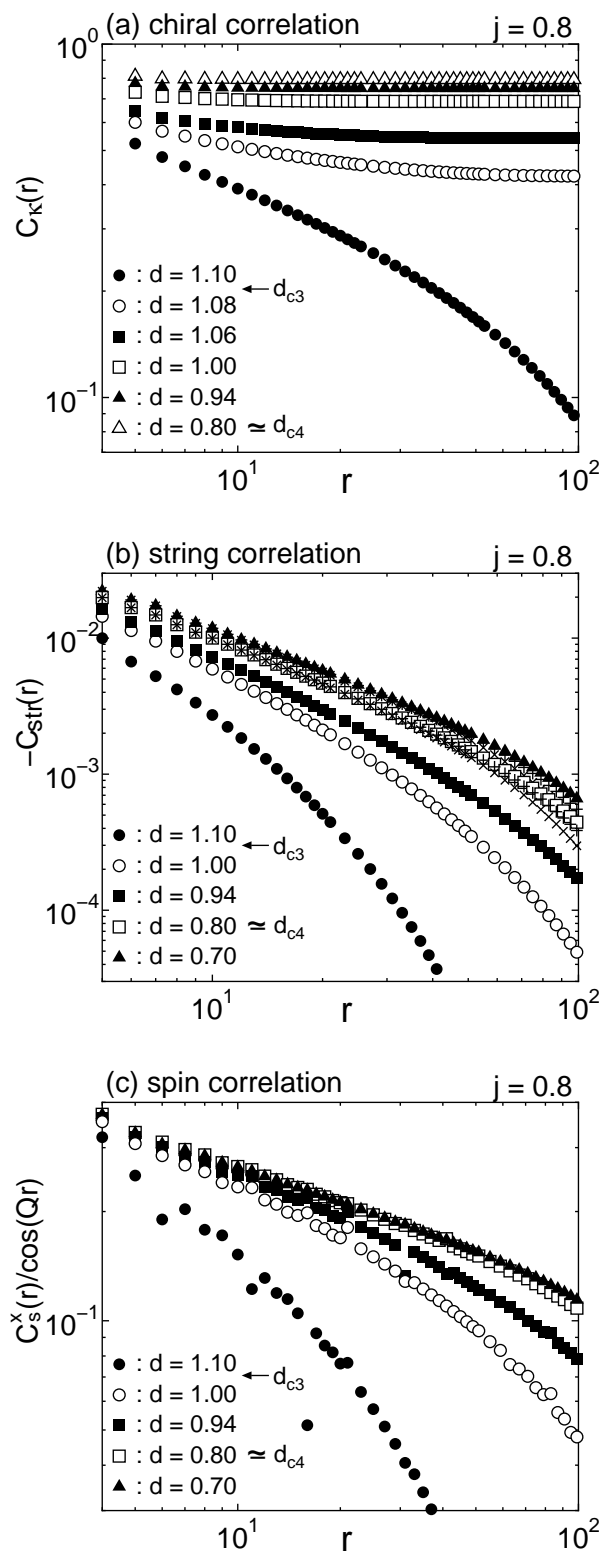


Fig.4, T.Hikihara



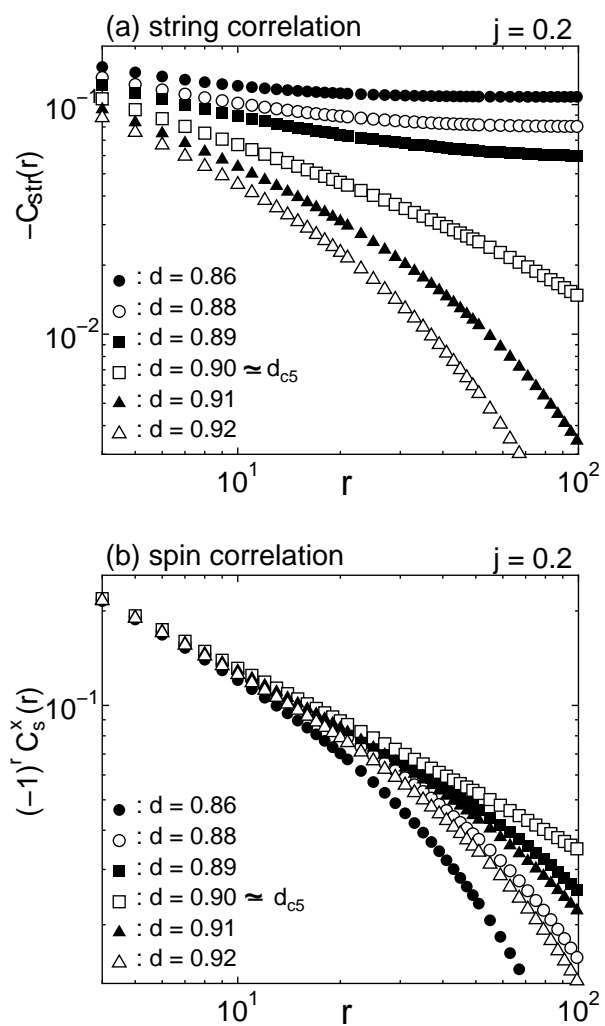


Fig.5, T.Hikihara

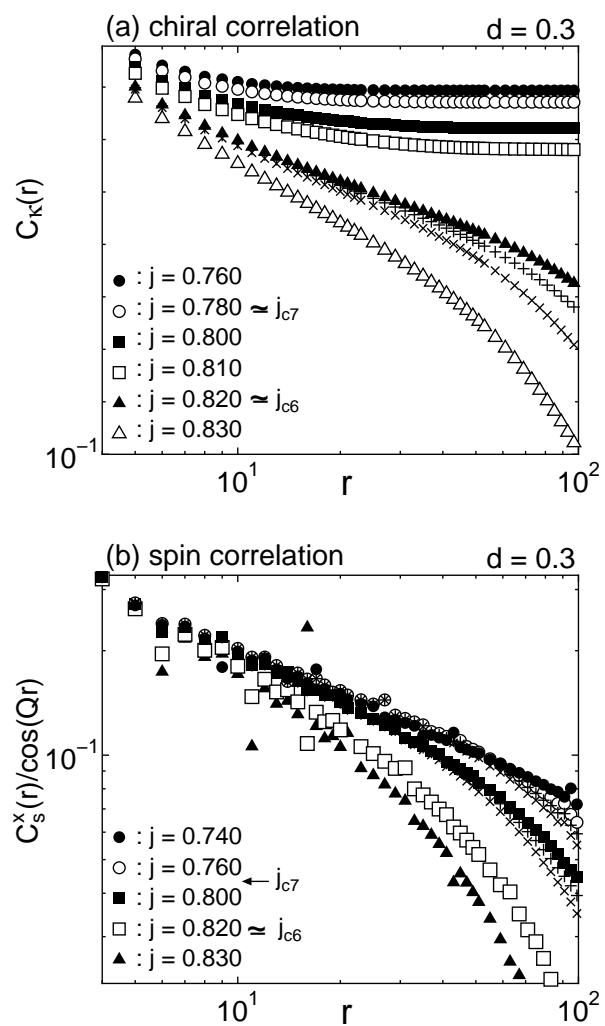


Fig.6, T.Hikihara

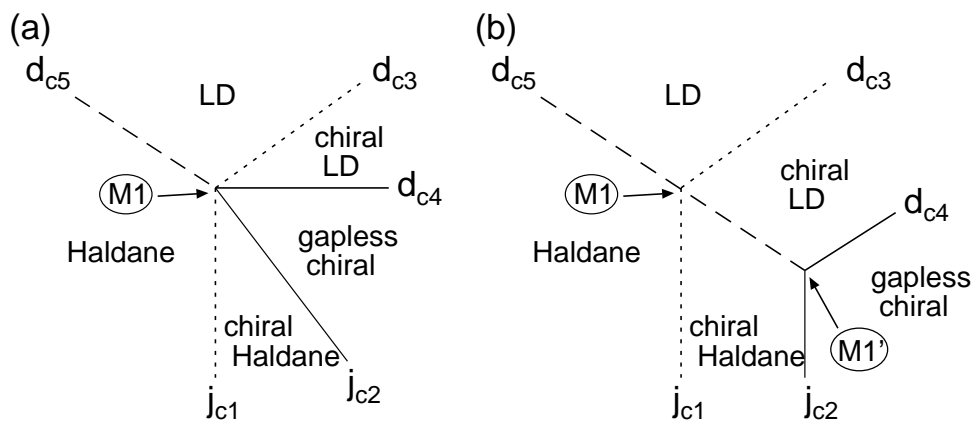


Fig.7, T.Hikihara